forests

MDPI

Article

The Effect of Rapid Development on Soil CO_2 Efflux in a Cellulosic Biofuel Stand

Nicholas Wright-Osment [1], Gregory Starr [1,*], Doug P. Aubrey [2,3], Benjamin M. Rau [4] and Christina L. Staudhammer [1]

[1] Department of Biological Sciences, University of Alabama, Tuscaloosa, AL 35487, USA
[2] Savannah River Ecology Laboratory, University of Georgia, Aiken, SC 29802, USA
[3] Warnell School of Forestry and Natural Resources, University of Georgia, Athens, GA 30602, USA
[4] USDA Forest Service Northern Research Station, Parsons, WV 26287, USA
* Correspondence: gstarr@ua.edu

Abstract: As awareness of climate change increases, the need for carbon neutral fuel sources is growing. Lignocellulosic biofuel derived from pine trees has been suggested as one potential energy source; however, it requires more research before its efficacy for climate change mitigation can be determined. Due to the large share of forest carbon held in soils and the extensive area of pine plantations in the southeast U.S., a better understanding of plantation soil carbon dynamics is critical for biofuel carbon accounting. This study evaluated the effects of canopy development and productivity on soil CO_2 efflux, a proxy for soil respiration (R_s), in an intensively managed loblolly pine (*Pinus taeda*) stand over a period from May 2015 to December 2019. We found that leaf area index (LAI) and gross ecosystem production (GEP), as well as meteorological variables, had significant effects on R_s, but that both overall R_s and soil carbon pools did not increase over the course of the study. We thus hypothesize that GEP and LAI had intra-annual effects on R_s, and that the lack of change in R_s is the result of an increase in autotrophic respiration (R_a) that offset a decrease in decomposition of the previous stand's organic matter.

Keywords: forest productivity; leaf area index; gross primary production; carbon; *Pinus taeda*

Citation: Wright-Osment, N.; Starr, G.; Aubrey, D.P.; Rau, B.M.; Staudhammer, C.L. The Effect of Rapid Development on Soil CO_2 Efflux in a Cellulosic Biofuel Stand. *Forests* **2023**, *14*, 258. https://doi.org/10.3390/f14020258

Academic Editor: Brian D. Strahm

Received: 21 December 2022
Revised: 26 January 2023
Accepted: 27 January 2023
Published: 30 January 2023

1. Introduction

Forest soil carbon (C) pools are a critical component of the global C budget as they account for two-thirds of all forest C and are estimated to be twice the size of the atmospheric carbon C sink [1–3]. These C pools are heavily impacted by human land conversion [4]; however, the severity and type of impact depends on how the land is manipulated. Typically, tree harvest reduces forest soil C concentrations [5,6]. The soil pool of previously harvested lands can be improved through reforestation [5,7]; however, the amount of time needed for C recovery in the soils is still unclear and appears to vary on a site-by-site basis, depending on forest type, and may be more than 50 years for southeastern forests [7–9].

The southeastern United States is an ideal location to study how soil C dynamics respond to forest land conversion, as the region has a history of deforestation and reforestation, and an extensive area of intensively managed pine plantations [10]. From the 1700s through the 1930s, the southeastern U.S. experienced widespread removal of old growth forests both for agricultural land and for logging [11,12]. After this period, natural reforestation of abandoned agriculture land, afforestation, and establishment of pine plantations once again changed the landscape. From 1952 to 2010, pine plantations went from being a negligible portion of southern forests to making up 19% of the forested area in the South [13]. Plantation establishment and an increasing emphasis on intensive silviculture [14,15] caused substantial increases in southern timber production from the 1950s to 2000 [10]. This trend is predicted to continue; by the year 2040, the area of southern pine plantations is projected to increase by at least 25% over 1995 levels [14].

No contemporary southern pine plantations are known to exist which have not undergone genetic modifications and/or selective breeding to maximize growth and productivity [16]. These faster-growing stands have accelerated physiological processes [14], but less is known about their soil C dynamics. It is well known that photosynthesis plays a critical role in soil carbon dioxide (CO_2) efflux, the release of CO_2 from the soil and is a proxy for soil respiration (R_s), in forests [17]. Swedish Scots pine forests, for instance, showed a 54% decline in R_s 1–2 months after girdling of all trees [17]. In addition, increased photosynthesis leads to increased production of photosynthate, a significant portion of which inevitably reaches the soil, both through vascular transport to the rhizosphere and through litterfall [18]. Researchers have also found a significant relationship between R_s and net primary production (NPP) [19,20], and Litton et al. [21] showed that R_s increases linearly with increasing gross primary production (GPP). It thus stands to reason that R_s should increase in stands modified to have accelerated growth. R_s is an integral component of broader ecosystem respiration (R_{eco}) and can account for between 45 and 80% of R_{eco} in forests [22,23]. Understanding the role of R_s in fast-growing pine forests of the southeastern U.S. will therefore provide key insights into both the components of R_{eco} and the movement of C.

While most commercial stands in the southeastern U.S. are planted to produce wood and paper products, a growing number of stands have been designated for biofuel feedstock plantations. There is still debate, however, over the economic and environmental viability of lignocellulosic biofuels and genetic modification to improve the efficiency and yield of stands [24]. Most research on such modifications has been conducted on transgenic poplar species; however, pines are another potential feedstock source [25]. The southeastern U.S. is seen as one potential region for the establishment of large-scale cellulosic biofuel production due to the extensive area of pine plantations [26]. *Pinus taeda* (loblolly pine) has been proposed as a possible species for use as a biofuels feed stock because of its rapid growth rate and prevalence [27–29]. Understanding the effects of management and tree improvement for enhanced biofuel production on soil C dynamics will prove critical to assessing the efficacy of these plantations in the context of reduction of greenhouse gas emissions.

Our study seeks to understand the effect of accelerated growth on the R_s of a young loblolly pine plantation intensively managed for biofuel feedstock. Within this study we will address the following questions: (1) How does rapid canopy development, as expressed by leaf area index (LAI), affect R_s. (2) What role does gross ecosystem production (GEP) play in controlling R_s rates?

2. Materials and Methods

2.1. Study Area

The study was conducted from June 2015 to December 2019 at the US Department of Energy, Savannah River Site (SRS), a National Environmental Research Park located on the Upper Coastal Plain physiographic region, near Aiken, South Carolina, U.S. The area is heterogenous, being characterized by ridges with sandy soils and floodplains and terraces with loamy soils. See White et al. for further site details [30]. The climate is humid subtropical with a long-term average annual air temperature of 17.6 °C [31]. Long-term average annual precipitation at the site is 1159 mm [31]. Before study establishment, the area was dominated by second rotation planted loblolly pines, which were established in 1951 following the abandonment of row-crop agriculture [32]. These stands were clear-cut in early 2012 and the site was subsequently prepared for watershed-scale experimental planting [33] aimed at determining the effects of intensive silviculture on soil and water quality. Bareroot seedlings specifically selected for high biomass production (ArborGen Mass Control Pollinated AGM 37) were planted between February and March 2013. The genetic source was identified to have 70% greater growth than the North Carolina State University Cooperative standard check source, with excellent stem form and rust resistance. The site went through a series of intensive herbicide, pesticide, and fertilizer applications

prior to and following planting. Details of these treatments can be found in Ferreira et al. (2020) [33].

2.2. Eddy Covariance Methodology

An eddy covariance tower was established on site in late January of 2015. Net ecosystem exchange (NEE), sensible energy (H), and latent energy (LE) were measured using the open-path eddy covariance (EC) method [34,35]. A control volume approach was applied to estimate NEE (μmol m^{-2} s^{-1}). This technique simplifies the continuity equation so that Integrals I and II (Equation (1)) represent the vertical rate of change of the mean molar CO_2 concentration and the vertical scalar flux divergence from ground level to the measurement height (z, m), respectively:

$$\mathrm{NEE} = \underbrace{\int_0^z \frac{\partial \rho C}{\partial t} \partial z}_{\mathrm{I}} + \underbrace{\int_0^z \frac{\partial \rho\, C'\, w'}{\partial t} \partial z}_{\mathrm{II}}, \quad (1)$$

where, ρ represents the dry air density. The CO_2 concentration (C, μmol m^{-3}) and vertical wind velocity (w, m s^{-1}) were measured at a fixed plane ~5 m above the mean canopy height. Meteorological conventions were used with negative values representing ecosystem C uptake. Primes indicate instantaneous fluctuations around the mean measured at 10 Hz while overbars denote the mean over the averaging period of 30 min. Due to the young age of the stand and low canopy height at the beginning of the study, the initial instrument height was 11.5 m and the zero-plane displacement estimate was changed monthly (due to the rapid accrual of canopy height) using the average heights of 20 randomly selected trees within the site. Typically, net ecosystem production (NEP) is defined as GEP − R_{eco} where GEP is gross ecosystem production (the overall influx of CO_2 into the system). In the case of our study C uptake was represented by a negative value while loss was represented by a positive value. Thus, NEP was defined as GEP + R_{eco} and negative values of GEP represented net uptake while positive values represented efflux from the system, per micrometeorological convention.

The concentrations of CO_2 and water vapor were measured with the open-path LI-7500-A infrared gas analyzer (IRGA, LI-COR Inc., Lincoln, NE, USA) and 3D sonic anemometer (CSAT-3, Campbell Scientific, Logan, UT, USA). The IRGA's optical path aligned to match the sampling volume of the 3D sonic anemometer. The instruments were separated by 0.23 m to minimize airflow distortion. A datalogger (CR3000, Campbell Scientific Inc., Logan, UT, USA) collected the raw data at 10 Hz. The IRGA was calibrated every 4 to 6 weeks using a known concentration of CO_2 gas (600 ppm ± 2%), dry N_2 gas scrubbed with soda lime and Drierite, and a dew point generator (LI-610, LI-COR Inc., Lincoln, NE, USA) as outlined in Ameriflux protocols [36,37].

2.3. Soil CO_2 Flux Measurement

Within the footprint of the eddy covariance tower, we established four 50 × 50 m plots, with each plot having five CO_2 flux collars. Monthly soil CO_2 flux measurements were taken on each soil collar within these monitoring plots (n = 20) using a static chamber approach with an infrared gas analyzer (LI-6400, LI-COR Inc., Lincoln, NE, USA). Measurements were taken between 10:00 and 14:00. Soil collars were made from polyvinyl chloride (PVC) rings (11.7 cm interior diameter and 4.4 cm height) and were placed ~1.0 m from the litterfall traps (described below). Live green biomass was carefully removed from each collar before performing measurements. Three replicate measurements were taken at each collar. Rate measurements were taken between −5 ppm and +5 ppm of the ambient CO_2 concentration. The first of these measurements was removed to assure stability within the

chamber and the other two were averaged. Soil CO_2 flux (R_s, μmol CO_2 m^{-2} s^{-1}) was calculated as:

$$R_s = \frac{kPV}{S(T_{air} + 273.15)} \left(\frac{\partial C}{\partial t} + \frac{C}{10^3 - W} \right) \frac{\partial W}{\partial t}, \quad (2)$$

where k = 10/8.314 = 1.2028; P is atmospheric pressure (kPa), V is the volume of the chamber (cm^3), S is the surface area covered by the chamber (cm^2), T_{air} is the ambient chamber air temperature as measured with the LI-6400 instrument (°C) at the soil surface, C and W are the molar ratio of carbon dioxide and water vapor in the chamber air, respectively (μmol CO_2 mol^{-1} air, and mmol H_2O mol^{-1} air), and t is the time (s). R_s was measured in μmol CO_2 m^{-2} s^{1} and converted to g CO_2 m^{-2} s^{-1}. For our analyses this was then scaled up to a daily value by multiplying the value by the number of seconds in a day (86,400), then further scaled up to a monthly value by multiplying the daily value by the number of days in the month. Thus, all non-transformed R_s values presented in the Results are in g CO_2 m^{-2} $month^{-1}$. Though this is a relatively rough estimate, it allows for full usage of our meteorological and flux data, which was taken every 30 min. In association with each R_s measurement, soil volumetric water content (VWC) in the top 20 cm of soil was measured (CS620, Campbell Scientific Inc., Logan, Utah) adjacent to the soil collar (<0.5 m). Soil temperatures were also measured at depths of 4 and 8 cm with insulated thermocouples (Type-T, Omega Engineering, Inc., Stamford, CT, USA).

2.4. Canopy Development

Canopy leaf area index (LAI) and canopy gap fraction measurements were taken monthly directly above each of the soil respiration collars using a digital camera with a hemispherical lens (Panasonic Lumix DMC-LX5, Regent Instruments, QC, Canada) at diameter at breast height (DBH; 1.34 m above ground level). Hemispherical photos were analyzed using Winscanopy V3.4 (Regent Instruments). Each photo was analyzed separately to calculate canopy LAI using the LI-COR LAI-2000 linear method. LAI values greater than 7 were discarded from analyses as such values are considered highly unrealistic and were associated with branches near the camera. Naturally regenerating *Liquidambar styraciflua* (American sweetgum) present in one subplot had a major impact on LAI values and we thus also discarded this subplot from analyses. A gap in data occurred from August to November 2017 because of equipment failure. LAI from this period is thus not included in statistical models described in Section 3.2.3.

Leaf litter was collected monthly from five 1 m^2 mesh traps suspended above the forest floor. Leaf litter traps were co-located with the soil respiration collars. Litter was placed in a paper bag and returned to the lab where it was dried to constant mass at 60 °C.

2.5. Soil Carbon Concentrations

As part of the watershed-scale experiment this study was nested within, eight replicate plots were established for monitoring soil responses to clear-cutting and subsequent stand development under intensive silviculture. Sampling locations were identified using unique combinations of random compass azimuth and random distance from plot center. At each sampling location within each plot a "bucket" type soil auger with an inside diameter of 8.26 cm and a height of 15 cm (AMS, American Falls, ID) was used to retrieve soil samples from four discrete depths (0–15, 15–30, 30–45, and 45–100 cm). Samples were composited by depth within each plot, placed in a plastic-lined bag and returned to the lab. All composite samples were dried at 60 °C for 48 h or until a constant weight was achieved. Dry samples were sieved to 2 mm then ground using a ball mill. Soils did not contain a measurable mass of >2 mm particles. All ground soil samples were sent to the USFS Coweeta Hydrologic Laboratory where they were analyzed for total C using a dry combustion Flash EA 1112 NC Analyzer (Elantech, Lakewood, NJ, USA).

To convert soil C concentration to total soil C mass (content) on an area basis (Mg ha^{-1}), three soil bulk density samples were collected from random locations within each plot using a volumetric soil corer with a removable 1002 cm^3 sleeve (AMS, Ameri-

can Falls, ID). Bulk density samples were collected from depths 0–15, 15–30, 30–45, and 45–60 cm, placed in a metal soil tin, and returned to the lab. All bulk density samples were dried at 105 °C until they achieved a constant weight. The mean dry soil bulk density was then calculated for each plot and depth increment. Soil C concentrations were multiplied by the corresponding dry soil bulk density and scaled to Mg ha^{-1}. Soil bulk density samples and soil chemistry samples were collected at the beginning of the experiment in February–March 2013 and again in May–June 2018. The first set of measurements were conducted at the site during replanting following clear-cutting. These measurements were part of our research team's larger Department of Energy Bioenergy Technologies Office project, which began prior to the establishment of our greenhouse gas measurements.

2.6. Statistical Analyses

A series of general linear mixed models (GLMM) was created to model R_s and its relationship with other variables using the *lme* package in the R statistical software [38]. Cursory testing revealed substantial heteroscedasticity and a lack of normality. To meet the assumptions underlying GLMM, the natural logarithm of R_s was used as the response variable in all models. GLMMs accounted for the random effect of year and plot. In addition, the models included a first-order autoregressive autocorrelation structure (AR(1)) to account for the repeated measures nature of monthly observations. The first GLMM solely modeled $\ln(R_s)$ as a function of LAI. With each subsequent model, a new micrometeorological variable and its interactive effects were incorporated. To avoid multicollinearity, highly correlated variables were not included together in the model. Each of these models was evaluated, and those variables or interactive effects which were not found to be significant ($p > 0.05$) were eliminated from the subsequent model; when interactive effects were significant, the underlying simple effects remained in the model. After creating a model including LAI and all other significant covariates, Akaike information criterion (AIC) scores were used to compare models. The model with the lowest AIC was assumed to best support the data. For all models, residuals were plotted to visually assess assumptions of homoscedasticity, and quantile–quantile plots were used to evaluate normality. In the final model, variables were considered significant if their *p*-values were below 0.05. Interaction plots were made with the *sjPlot* package [39].

To determine if there were significant differences in soil C stock location between 2013 and 2018, the soil C stock data was analyzed using a series of t-tests. Tests for the difference of two means (2018 vs. 2013) were performed for each depth between the sampling periods. These tests were performed on soil C values averaged across all plots ($n = 8$ for each depth in each year).

3. Results

3.1. Site Conditions

In the two years of the study, the average air temperature (T_{air}) was greater than the site historical average of 17.6 °C [31]. Average T_{air} over the course of the study was 19.2 °C with the highest annual average occurring in 2015 (22.8 °C) and the lowest occurring in 2018 (17.7 °C) (Figure 1).

In 2018, total rainfall was substantially higher than in any other year (1406 mm). Additionally, it was the only full year of the study in which the total rainfall surpassed the site historical average of 1159 mm [31]. In 2016, 2017, and 2019, the study site experienced below average rainfall (1011, 981, and 1146 mm, respectively) (Figure 2). Note, that measurements in 2015 began in March and are thus not a complete representation of the year.

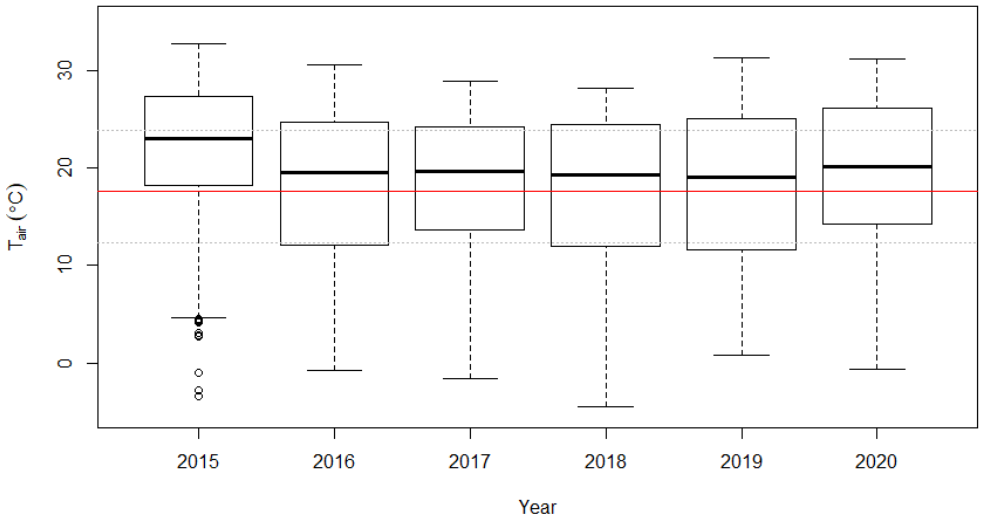

Figure 1. Average air temperature for each year over the course of the study. The red line represents the historical average temperature of the area (17.6 °C) [31] and the grey lines represent current average daily high and low temperatures.

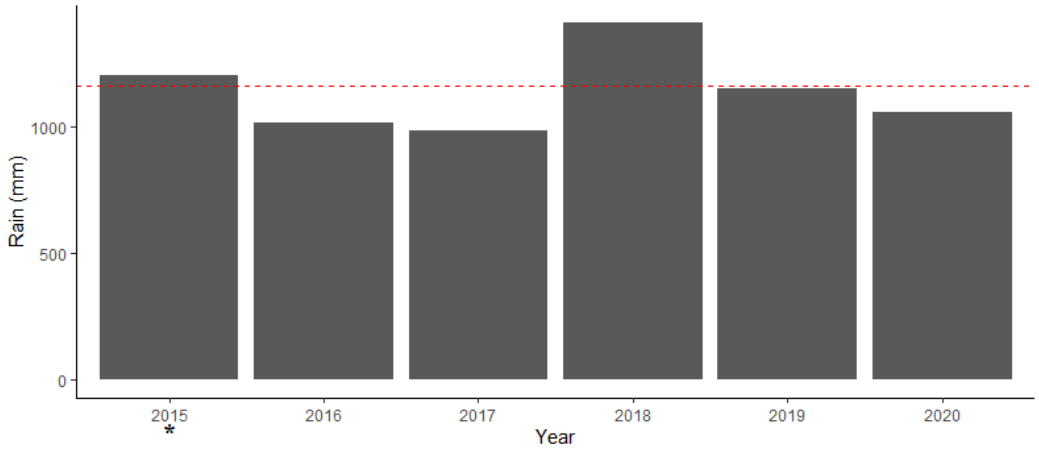

Figure 2. Total rainfall for each year over the course of the study. The red line represents 1406 mm, the historical average annual rainfall for the area [31]. * Measurements in 2015 began in March and do not represent a complete year.

3.2. Soil Respiration and Stand Development

3.2.1. R_s over the Study Period

R_s showed clear seasonal variation, with peak R_s occurring in summer and the lowest values in the winter (Figure 3). Additionally, there was little change in the mean of R_s (2.304 ± 1.448 µmol CO_2 m^{-2} s^{-1}, or a scaled-up 71.72 ± 45.07 g CO_2 m^{-2} $month^{-1}$) over the course of the study.

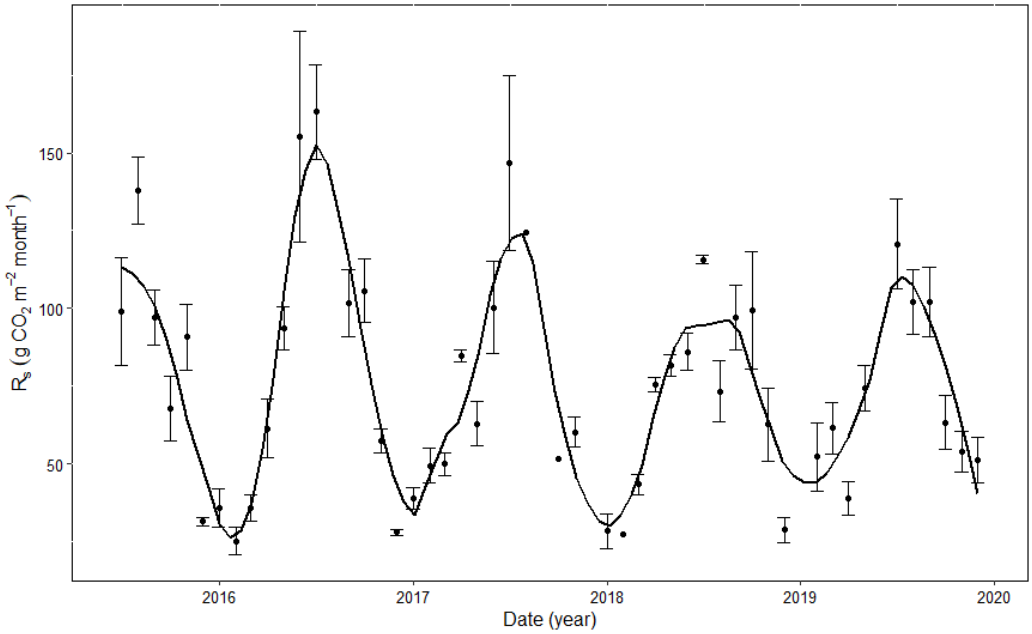

Figure 3. Monthly mean measured rate of R_s over the course of the study period. Curve generated via locally estimated scatterplot smoothing (LOESS) method.

3.2.2. Canopy Development

On average, LAI increased over the course of the study (Figure 4). A pronounced intra-annual pattern was observed, with LAI peaking in the summer months as would be expected. The decline in LAI during 2019 was associated with two tropical storms passing the site during fall 2018. This removed canopy needles that would have been retained until the fall of 2019 based on leaf phenological characteristics of loblolly pine.

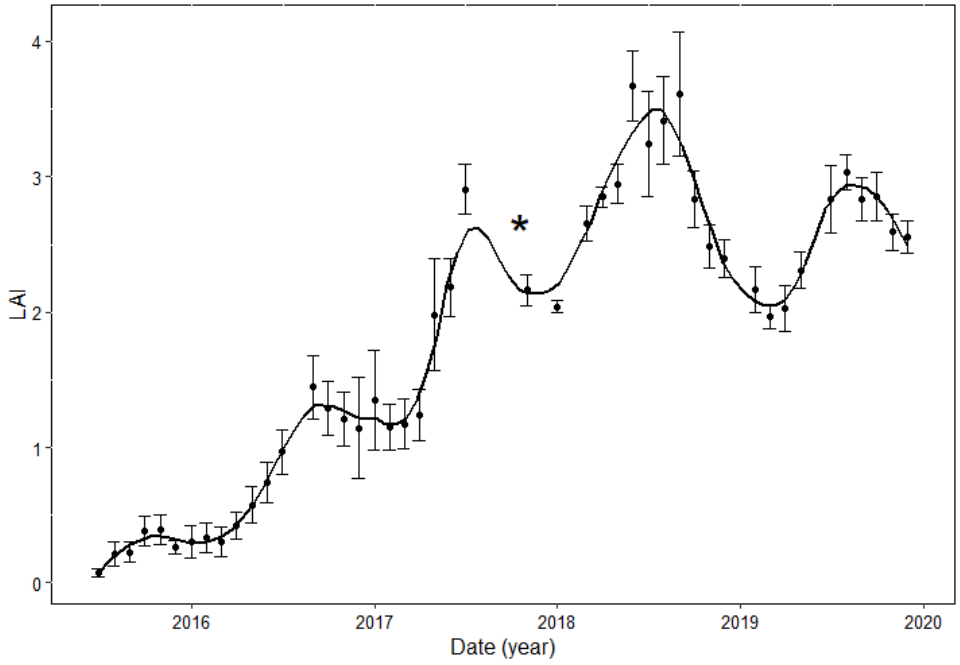

Figure 4. LAI over the course of the study. * The gap in data from August to November of 2017 was the result of broken equipment. Curve generated via locally estimated scatterplot smoothing (LOESS) method.

3.2.3. Models Relating R_s, LAI, and Other Predictors

Linear mixed effects models were created to determine the relationship between R_s, LAI, and micrometeorological variables collected at the site (Table 1). Preliminary model results, which relied solely on LAI as the predictor variable, indicated that assumptions of normality and homoscedasticity were met. This model indicated that there was a strong, positive relationship between LAI and R_s ($p < 0.0001$).

Table 1. Estimated fixed effects, degrees of freedom, and statistical test for linear mixed models of $\ln(R_s)$.

Model	AIC	Effect	NumDF	DenDF	Estimate	F-Value	*p*-Value
preliminary	1519	LAI	1	726	0.135158	22.224	<0.0001
final	892	LAI	1	512	−0.034164	20.892	<0.0001
		VWC	1	512	−0.018537	109.94	<0.0001
		Tair	1	512	0.043412	91.869	<0.0001
		GEP	1	512	0.001961	262.60	<0.0001
		VPD	1	512	0.515418	2.625	0.1058
		VWC × Tair	1	512	0.001628	10.504	0.0013
		GEP × VPD	1	512	−0.005794	1.800	0.1803
		Tair × VPD	1	512	−0.045823	9.772	0.0019
		VWC × VPD	1	512	−0.075488	19.284	<0.0001

The final (lowest AIC) model of R_s included LAI, monthly GEP, T_{air}, VWC, vapor pressure deficit (VPD), the interaction of VWC with T_{air}, and the interactions of VPD with VWC, with monthly GEP, and with T_{air} ($p \leq 0.001$; Table 1). Despite having a significant effect on R_s in the preliminary model, when all other variables were taken into account in the final model, LAI had a small negative effect on R_s; R_s decreased slightly with increasing LAI, given VWC, T_{air}, GEP, and VPD were already in the model. There was a similar relationship between R_s and both VWC and GEP. T_{air}, on the other hand, had a positive effect, increasing R_s. The magnitude of all these effects, along with the interactive effects, however, was very low. Though VPD alone did not have a significant effect on R_s, it proved to have an interactive effect with a variety of other variables, moderating the effects of GEP and VWC, and amplifying the effect of T_{air} (Table 1).

While R_s decreased with increasing VWC, the magnitude of the decrease was larger at lower T_{air} (Figure 5). Changes in VPD also affected the magnitude of the effects of GEP, VWC, and T_{air} on R_s. The most notable of these interactions was that of VPD and GEP. While GEP had no significant relationship with R_s when VPD was lower (0.41 kPa), as VPD increased (0.8 kPa), higher VPD resulted in more strongly decreased R_s. VWC showed a similar relationship with R_s over VPD values, with no significant relationship between VWC and R_s at low VPD and decreasing R_s with VWC at higher values of VPD. Finally, T_{air} had a positive impact on R_s, which was more pronounced at low VPD values.

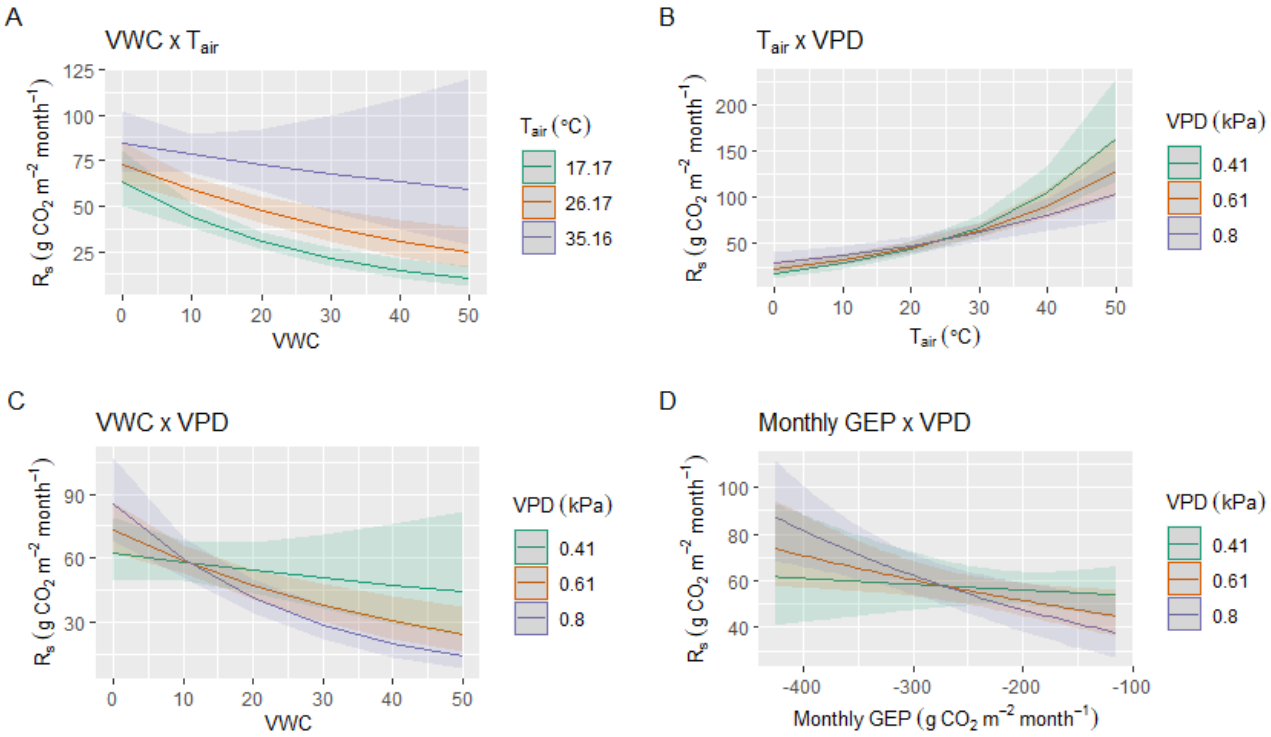

Figure 5. Estimated marginal mean R_s values from final linear model, (**A**): by VWC (%) and T_{air} (°C), (**B**): by T_{air} and VPD (kPa), (**C**): by VWC and VPD, and (**D**): by GEP (g CO_2 m^{-2} $month^{-1}$) and VPD.

3.3. Soil Carbon Stocks

Soil Carbon

Overall, soil C stocks at the site decreased at all depths except 0–15 cm (Figure 6). Soil C stocks from 0–15 cm below ground increased by 4.418 Mg ha^{-1} between 2013 and 2018. However, statistical tests revealed no significant differences in C stock between the two years for each soil depth, thus suggesting that the changes were not different by year. In addition, the overall mean soil C content between the two years was highly similar: 14.896 Mg C ha^{-1} in 2013 and 14.947 Mg C ha^{-1} in 2018.

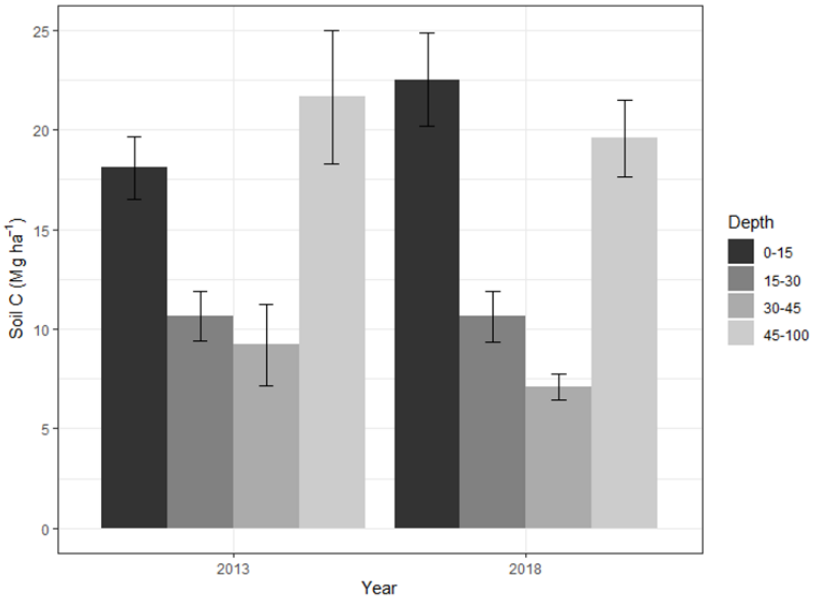

Figure 6. Soil carbon stocks (Mg ha^{-1}) at four depths in 2013 and 2018. Error bars represent ± one standard error.

4. Discussion

As expected, LAI had a significant relationship with R_s. Though its proportion varies substantially among different systems [40], autotrophic respiration (R_a), the respiration of plants and associated symbiotic organisms, has been shown to be a major contributor to R_s in coniferous forests [17,22,41]. R_a is directly influenced by recent photosynthesis [17,42–44] because photosynthates are broken down to provide energy for both the tree itself and the associated symbiotic organisms. LAI is an established proxy for photosynthetic productivity [45]; thus it is reasonable that it would have a significant relationship with R_s. R_s, however, experienced little increase over the course of the study (Figure 3) while LAI saw a net increase (Figure 4). This does not align with other studies of coniferous forests, which show a positive linear relationship between LAI and R_s [21,46]. This study suggests that, in the context of the SRS pine stand, LAI's significance is primarily due to intra-annual (seasonal) effects on R_s. Further evidence for the dominance of a seasonal effect is revealed by the low coefficient of LAI in all models, and the reversal in direction of this effect when micrometeorological variables were added to the model. Though considered "evergreen", coniferous forests contain maximum foliage during the growing season, when productivity is the highest. Thus, LAI likely affects R_s because of its relationship to increased photosynthesis in the warmer months. Supporting this conclusion, GEP also had a highly significant impact on R_s despite having a low regression coefficient. Throughout the study GEP experienced an interannual decline, meaning more carbon entered the system, as LAI increased; however, the relationship with R_s again appears to be primarily driven by seasonality.

As productivity increased in the growing stand, why did we not observe a corresponding increase in R_s? It is possible that the answer lies in the relative contributions of heterotrophic and autotrophic respiration (R_h and R_a) to overall R_s. Assuming R_a is increasing with productivity [17,42–44], the lack of change in overall R_s might be attributable to an offsetting decrease in R_h, as time since the previous clear-cut increases. Despite the lack of overall change and the insignificance of the t-tests, the pattern in soil C pool over time (Figure 6) may support this theory. From 2013 to 2018, these data show an increase in soil C from 0–15 cm and a decrease in soil C from 45–100 cm. The increase at the shallowest depths could correspond to the accumulation of new belowground biomass as well as increased litter deposition as the stand grows. The loss of C at the lowest depths, on the other hand, may be the result of continuing decomposition of legacy organic matter, such as roots, from the previous forest, which was clear-cut in 2012. It is possible that, as decomposition occurred, soil decomposers were forced to consume more recalcitrant substrates, leading to a reduction in R_h from the deep soil. When we began sampling R_s in 2015, R_h may have been higher than it was in 2019 and R_a may have been lower. It is also possible that the increase in soil C at the highest stratum corresponds instead to the incorporation of C from decomposition of surface detritus from the previous stand. From the period directly after harvest to 2017 we observed both a substantial decrease in the amount of detritus (woody and foliar) from the previous stand and the formation of a new mat of pine needles (Rau, personal observation). Not only might this have elevated C from 0–15 cm, but high decomposition may have inflated R_s early in the study through a corresponding high R_h. No matter the source of the carbon, these scenarios suggest an initial high R_h which decreased as detritus from the previous stand decomposed and an initially low R_a which increased at a corresponding rate as the stand became more productive. This theory aligns well with the findings of other shorter-term studies that R_s following clear-cut is not significantly different from R_s in adjacent mature stands [47,48]. Perhaps R_h from decomposition post-clear-cut is comparable to the combined R_a and R_h of mature forests.

Alternatively, as a new stand develops, R_s should be mainly from R_a because fine root production increases for the first 3–5 years and then plateaus (much like LAI). Fine root mortality is almost nonexistent until year three or four. In approximately year 4, fine root production and mortality are equivalent [49]. Of course, this only accounts for the newly planted trees, while decomposition from the previous old stand is likely dominating

below-ground respiration. We also did not measure the potential of respired CO_2 being transported through the xylem, which was outside the scope of this study. It is well known that as LAI increases with stand development so does transpiration [50], which could have led to R_a bypassing soil respiration [51,52].

Our study also aligns with previous literature in the conclusion that both VWC and T_{air} have a significant effect on R_s [53,54]. The interactive effect of VWC and T_{air} on R_s has been reported previously in pine forests, showing that R_s becomes less sensitive to T_{air} at low VWC [55]. We also found that R_s was more sensitive to changes in VWC when VWC was lower, but this pattern became less apparent at higher T_{air}. There instead appears to be a negative linear relationship between R_s and VWC at higher temperatures. Other studies have shown a positive linear relationship between temperature and R_s [56] while ours shows a positive—though curvilinear—effect, with the slope of the relationship increasing more rapidly at higher T_{air}. Overall, the positive association between T_{air} and R_s is reasonable as respiration is a chemical process which would logically be influenced by simple thermodynamics. The simple effect of VWC on R_s, on the other hand, has been shown to vary extensively by region and by scale and is difficult to generalize [56,57]. Our study corroborates the conclusion of Hursh et al. [56] that VWC is especially influential on R_s in temperate evergreen forests. In our *P. taeda* plantation, VWC was negatively related to R_s at all T_{air} values —a relationship also reported in a longleaf pine savannah in the U.S. Southeast [58]. The negative relationship could be due to inhibition of diffusive processes. Higher VWC may be slowing the speed with which CO_2 from respiration is able to diffuse out of the soil. It is also possible that higher VWC is leading to the creation of anoxic areas where O_2 cannot be used as the terminal electron acceptor for respiration. Less efficient forms of respiration may thus occur when VWC is higher, promoting a decrease in the rate of CO_2 efflux.

The relationship of VPD with all these variables is intriguing. While VPD did not have a significant simple effect on R_s, changes in VPD appear to impact the magnitude of the relationship between all the predictor variables (excluding LAI) and R_s. A lower VPD enhances the impact of increasing T_{air}, while a higher VPD amplifies the effect of changes in GEP and VWC. The interaction plot of R_s as a function of T_{air} and VPD appears to suggest somewhat consistent responses of R_s to T_{air} (increasing as expected) at lower temperatures; however, VPD plays a larger role at higher T_{air}, with lower VPD leading to more rapid increases in R_s. This is likely related to R_a and, by extension, photosynthesis. To a point, photosynthesis is known to increase with temperature; however, drought stress can prove limiting to a plant's ability to continue photosynthesizing due to the closing of stomata [59,60]. At low drought stress (indicated by low VPD) it is likely that the trees are able to maintain stomatal conductance [59,61] and by extension, enhanced productivity. This would stimulate an increase in R_a [17,42–44] which, in turn, would naturally lead to an increase in overall R_s [22]. Explaining the interactive effects of GEP and VWC with VPD is more challenging. It stands to reason that VWC would be lower with higher VPD, as more soil water would be lost to evaporation; however, it also appears that higher VPD values promote a more negative relationship between R_s and VWC. This is the inverse of the pattern that was seen with T_{air} and VWC, whereby higher T_{air} led to a dampened relationship. At low VPD, the relationship between GEP and R_s was negligible if not slightly positive, while high VPD produced a clear negative and increasing relationship between GEP and R_s, with higher GEP (less productivity) leading to lower R_s. The simple relationship between GEP and R_s here is reasonable in the context of R_a, and the VPD effect may make sense in the context of soil water loss. At higher VPD, the rate of transpiration from the canopy will likely increase. This increase in transpiration would place more water demand on the soil, especially around roots, and could produce a decrease in VWC. The negative relationship between VWC and R_s might produce higher soil efflux at high GEP, compounding the effect of GEP on R_a. Though it does not have a simple effect on R_s, the array of indirect effects of VPD make it a critical consideration for soil efflux at our site.

Because of the likely variation in the source of the soil respiration, the relationship between soil respiration and LAI would likely be substantially different had the stand been planted after the previous clear-cut's detritus was allowed to degrade. Thus, this study does not provide a quality characterization of how soil respiration would be affected were the selectively bred *P. taeda* to be planted for reforestation/afforestation of unforested land which was in relative equilibrium and had not been recently manipulated. However, this research does provide insight into the effect of clear-cutting then relatively rapid planting on the soil carbon dynamics of pine plantations, a more likely scenario. Accounting for soil flux from the previous stand's carbon stocks will be critical in accurately modeling the carbon sequestration potential of rapid-turnover pine plantations. In order to model and evaluate C dynamics in pine stands for biofuel production, further studies which quantify soil C stocks at various depths, and which parse out R_s into its heterotrophic and autotrophic components will be critical. In addition, more work is needed which follows carbon, at various scales, in pine stands before and after clear-cut and for many years as the next stand regenerates. This research is critical in the context of plantations like ours, which have been selectively bred for higher productivity, quicker growth, and, by extension, shorter rotation times. Under standard harvest practices, quicker rotations imply more clear-cut events in the same period. C dynamics cannot be studied in isolation however, and such studies must also follow the standard swathe of meteorological variables both atmospheric and soil-level.

It is vital to note some critical limitations to our study. First, we were unable to record soil flux at the same frequency as atmospheric flux. Our soil respiration data was based on two measurements from each subplot (n = 40) taken once monthly during peak hours. We scaled this up to monthly intervals, but this likely overestimated the true soil flux in each month. Thus, any results presented are implicitly following peak soil flux, not overall soil flux. In addition, our soil carbon stock estimates come from only one measurement period in 2013 and one in 2018. More frequent C stock measurements would have enhanced our ability to draw conclusions about the movement of carbon in belowground pools.

5. Conclusions

Overall, both LAI and GEP proved to be significant predictors of R_s; however, this significance was seasonal in nature and there was no net change in R_s over our five years of observation. This result may be the result of high R_h from decomposition of the previous stand's litter which was gradually replaced by R_a from the growing stand; however, without explicit data parsing out these two components, this conclusion is only conjecture. T_{air} and VWC also proved to be important predictors of R_s, aligning well with previous literature, though the impact of each was affected both by the other and by VPD. Despite exerting no direct control, VPD appears to be an important indirect regulator of R_s. For pine plantations for biofuel production to be considered a valid method of mitigating climate change, inter-rotational carbon dynamics must be studied, especially as trees are engineered or bred to grow faster and have shorter rotation periods. Such studies will improve carbon accounting and modeling, strengthen life cycle analyses, and help to inform landholders as to how best to manage detritus from clear-cuts.

Author Contributions: G.S., D.P.A. and B.M.R. acquired funding to conduct this study. G.S., D.P.A., B.M.R. and N.W.-O. contribute to data collection and data curation. C.L.S., N.W.-O., D.P.A. and G.S. contributed to data analyses. All authors contributed to the development and writing of the manuscript. All authors have read and agreed to the published version of the manuscript.

Funding: This research was funded by the Department of Biological Sciences at the University of Alabama and the Department of Energy–Savannah River Operations Office through the U.S. Forest Service–Savannah River under Interagency Agreement DE-AI09-00SR22188 and from the U.S. Department of Energy's Bioenergy Technologies Program to Oak Ridge National Laboratory. Oak Ridge National Laboratory is managed by UT-Battelle, LLC, for the U.S. Department of Energy under contract DE-AC05-00OR22725. This material is also based upon work supported by the Department

of Energy under award number DE-EM0004391 to the University of Georgia Research Foundation and McIntire Stennis project 1023985 from the USDA National Institute of Food and Agriculture.

Data Availability Statement: Data from this study can be found on Figshare.

Acknowledgments: We thank J. Arnold, B. Blackburn, J. Blake, H. Davis, H. Forehand, A. Horcher, R. Sutton, and C. Trettin for their contributions and support.

Conflicts of Interest: The authors declare no conflict of interest.

References

1. Schimel, D.S. Terrestrial ecosystems and the carbon cycle. *Glob. Chang. Biol.* **1995**, *1*, 77–91. [CrossRef]
2. Pan, Y.; Birdsey, R.A.; Fang, J.; Houghton, R.; Kauppi, P.E.; Kurz, W.A.; Phillips, O.L.; Shvidenko, A.; Lewis, S.L.; Canadell, J.G.; et al. A Large and Persistent Carbon Sink in the World's Forests. *Science* **2011**, *333*, 988–993. [CrossRef]
3. Dixon, R.K.; Solomon, A.M.; Brown, S.; Houghton, R.A.; Trexier, M.C.; Wisniewski, J. Carbon Pools and Flux of Global Forest Ecosystems. *Science* **1994**, *263*, 185–190. [CrossRef]
4. Lal, R. Forest soils and carbon sequestration. *For. Ecol. Manag.* **2005**, *220*, 242–258. [CrossRef]
5. Akala, V.A.; Lal, R. Soil Organic Carbon Pools and Sequestration Rates in Reclaimed Minesoils in Ohio. *J. Environ. Qual.* **2001**, *30*, 2098–2104. [CrossRef]
6. Nave, L.E.; Vance, E.D.; Swanston, C.W.; Curtis, P.S. Harvest impacts on soil carbon storage in temperate forests. *For. Ecol. Manag.* **2010**, *259*, 857–866. [CrossRef]
7. Silver, W.L.; Ostertag, R.; Lugo, A.E. The Potential for Carbon Sequestration through Reforestation of Abandoned Tropical Agricultural and Pasture Lands. *Restor. Ecol.* **2000**, *8*, 394–407. [CrossRef]
8. Chen, Y.; Yu, S.; Liu, S.; Wang, X.; Zhang, Y.; Liu, T.; Zhou, L.; Zhang, W.; Fu, S. Reforestation makes a minor contribution to soil carbon accumulation in the short term: Evidence from four subtropical plantations. *For. Ecol. Manag.* **2017**, *384*, 400–405. [CrossRef]
9. Paul, K.I.; Polglase, P.J.; Richards, G.P. Predicted change in soil carbon following afforestation or reforestation, and analysis of controlling factors by linking a C accounting model (CAMFor) to models of forest growth (3PG), litter decomposition (GENDEC) and soil C turnover (RothC). *For. Ecol. Manag.* **2003**, *177*, 485–501. [CrossRef]
10. Wear, D.N.; Greis, J.G. Southern Forest Resource Assessment: Summary of Findings. *J. For.* **2002**, *100*, 6–14. [CrossRef]
11. Steyaert, L.T.; Knox, R.G. Reconstructed historical land cover and biophysical parameters for studies of land-atmosphere interactions within the eastern United States. *J. Geophys. Res.* **2008**, *113*, D02101. [CrossRef]
12. Waisanen, P.J.; Bliss, N.B. Changes in population and agricultural land in conterminous United States counties, 1790 to 1997. *Glob. Biogeochem. Cycles* **2002**, *16*, 84-1–84-19. [CrossRef]
13. Wear, D.N.; Greis, J.G. *The Southern Forest Futures Project: Summary Report*; Gen Tech Rep SRS-GTR-168; USDA-Forest Service, Southern Research Station: Asheville, NC, USA, 2012; Volume 168, pp. 1–54. Available online: https://www.fs.usda.gov/treesearch/pubs/42526 (accessed on 7 July 2022).
14. Prestemon, J.P.; Abt, R.C. Southern Forest Resource Assessment highlights: The Southern Timber Market to 2040. *J. For.* **2002**, *100*, 16–22. [CrossRef]
15. Lee Allen, H.; Fox, T.R.; Campbell, R.G. What is Ahead for Intensive Pine Plantation Silviculture in the South? *South. J. Appl. For.* **2005**, *29*, 62–69. [CrossRef]
16. McKeand, S.; Mullin, T.; Byram, T.; White, T. Deployment of Genetically Improved Loblolly and Slash Pines in the South. *J. For.* **2003**, *101*, 32–37. [CrossRef]
17. Högberg, P.; Nordgren, A.; Buchmann, N.; Taylor, A.F.S.; Ekblad, A.; Högberg, M.N.; Nyberg, G.; Ottosson-Löfvenius, M.; Read, D.J. Large-scale forest girdling shows that current photosynthesis drives soil respiration. *Nature* **2001**, *411*, 789–792. [CrossRef]
18. Brüggemann, N.; Gessler, A.; Kayler, Z.; Keel, S.G.; Badeck, F.; Barthel, M.; Boeckx, P.; Buchmann, N.; Brugnoli, E.; Esperschütz, J.; et al. Carbon allocation and carbon isotope fluxes in the plant-soil-atmosphere continuum: A review. *Biogeosciences* **2011**, *8*, 3457–3489. [CrossRef]
19. Raich, J.W.; Schlesinger, W.H. The global carbon dioxide flux in soil respiration and its relationship to vegetation and climate. *Tellus B* **1992**, *44*, 81–99. [CrossRef]
20. Chen, S.; Zou, J.; Hu, Z.; Chen, H.; Lu, Y. Global annual soil respiration in relation to climate, soil properties and vegetation characteristics: Summary of available data. *Agric. For. Meteorol.* **2014**, *198–199*, 335–346. [CrossRef]
21. Litton, C.M.; Raich, J.W.; Ryan, M.G. Carbon allocation in forest ecosystems. *Glob. Chang. Biol.* **2007**, *13*, 2089–2109. [CrossRef]
22. Högberg, P.; Nordgren, A.; Högberg, M.N.; Ottosson-Löfvenius, M.; Singh, B.; Olsson, P.; Linder, S. Fractional contributions by autotrophic and heterotrophic respiration to soil-surface CO_2 efflux in Boreal forests. In *The Carbon Balance of Forest Biomes*; Griffith, H., Jarvis, P., Eds.; Taylor & Francis: London, UK, 2005; pp. 251–267.
23. Davidson, E.A.; Janssens, I.A.; Luo, Y. On the variability of respiration in terrestrial ecosystems: Moving beyond Q10. *Glob. Chang. Biol.* **2006**, *12*, 154–164. [CrossRef]
24. Bryant, N.D.; Pu, Y.; Tschaplinski, T.J.; Tuskan, G.A.; Muchero, W.; Kalluri, U.C.; Yoo, C.G.; Ragauskas, A.J. Transgenic Poplar Designed for Biofuels. *Trends Plant Sci.* **2020**, *25*, 881–896. [CrossRef] [PubMed]

25. Haile, S.; Palmer, M.; Otey, A. Potential of loblolly pine: Switchgrass alley cropping for provision of biofuel feedstock. *Agrofor. Syst.* **2016**, *90*, 763–771. [CrossRef]
26. Perdue, J.H.; Stanturf, J.A.; Young, T.M.; Huang, X.; Dougherty, D.; Pigott, M.; Guo, Z. Profitability potential for *Pinus taeda* L. (loblolly pine) short-rotation bioenergy plantings in the southern USA. *For. Policy Econ.* **2017**, *83*, 146–155. [CrossRef]
27. Peter, G.F. Southern Pines: A Resource for Bioenergy. In *Genetic Improvement of Bioenergy Crops*; Vermerris, W., Ed.; Springer: New York, NY, USA, 2008. [CrossRef]
28. Smith, W.B.; Miles, P.D.; Perry, C.H.; Pugh, S.A. Data CD Coord. 2009 Forest Resources of the United States. 2007. Available online: https://www.srs.fs.usda.gov/pubs/17334 (accessed on 16 July 2022).
29. Kline, K.L.; Coleman, M.D. Woody energy crops in the southeastern United States: Two centuries of practitioner experience. *Biomass Bioenergy* **2010**, *34*, 1655–1666. [CrossRef]
30. White, D.L.; Gaines, K.F. The Savannah River Site: Site description, land use, and management history. *Stud. Avian Biol.* **2000**, *21*, 8–17.
31. Weinbeck, S.W.; Viner, B.J.; Rivera-Giboyeaux, A.M. *Meteorological Monitoring Program at the Savannah River Site*; SRNL-STI-2020-00197; Savannah River National Lab: Aiken, SC, USA, 2020; pp. 1–138. Available online: https://srnl.doe.gov/atg/static/pdf/SRNL-TR-2020-00197.pdf (accessed on 2 June 2022).
32. Aubrey, D.P.; Blake, J.I.; Zarnoch, S.J. From Farms to Forests: Landscape Carbon Balance after 50 Years of Afforestation, Harvesting, and Prescribed Fire. *Forests* **2019**, *10*, 760. [CrossRef]
33. Ferreira, G.W.D.; Rau, B.M.; Aubrey, D.P. Herbicide, fertilization, and planting density effects on intensively managed loblolly pine early stand development. *For. Ecol. Manag.* **2020**, *472*, 118206. [CrossRef]
34. Ocheltree, T.W.; Loescher, H.W. Design of the AmeriFlux Portable Eddy Covariance System and Uncertainty Analysis of Carbon Measurements. *J. Atmos. Ocean. Technol.* **2007**, *24*, 1389–1406. [CrossRef]
35. Moncrieff, J.B.; Massheder, J.M.; de Bruin, H.; Elbers, J.; Friborg, T.; Heusinkveld, B.; Kabat, P.; Scott, S.; Soegaard, H.; Verhoef, A. A system to measure surface fluxes of momentum, sensible heat, water vapour and carbon dioxide. *J. Hydrol.* **1997**, *188–189*, 589–611. [CrossRef]
36. Munger, J.W.; Loescher, H.W. Preface to special section on new approaches to quantifying exchanges of carbon and energy across a range of scales. *J. Geophys. Res.* **2006**, *111*, D14S91. [CrossRef]
37. Munger, J.W.; Loescher, H.W.; Luo, H. Measurement, Tower, and Site Design Considerations. In *Eddy Covariance: A Practical Guide to Measurement and Data Analysis*; Aubinet, M., Vesala, T., Papale, D., Eds.; Springer: Dordrecht, The Netherlands, 2012; pp. 21–58.
38. R Core Team. *R: A Language and Environment for Statistical Computing*; R Foundation for Statistical Computing: Vienna, Austria, 2019; Available online: https://www.R-project.org/ (accessed on 5 January 2022).
39. Lüdecke, D. sjPlot: Data Visualization for Statistics in Social Science. R Package Version 2.8.8. 2021. Available online: https://CRAN.R-project.org/package=sjPlot (accessed on 13 January 2022).
40. Kukumägi, M.; Ostonen, I.; Uri, V.; Helmisaari, H.; Kanal, A.; Kull, O.; Lõhmus, K. Variation of soil respiration and its components in hemiboreal Norway spruce stands of different ages. *Plant Soil* **2017**, *414*, 265–280. [CrossRef]
41. Matteucci, M.; Gruening, C.; Goded Ballarin, I.; Seufert, G.; Cescatti, A. Components, drivers and temporal dynamics of ecosystem respiration in a Mediterranean pine forest. *Soil Biol. Biochem.* **2015**, *88*, 224–235. [CrossRef]
42. Hopkins, F.; Gonzalez-Meler, M.; Flower, C.E.; Lynch, D.J.; Czimczik, C.; Tang, J.; Subke, J. Ecosystem-level controls on root-rhizosphere respiration. *New Phytol.* **2013**, *199*, 339–351. [CrossRef]
43. Högberg, P.; Read, D.J. Towards a more plant physiological perspective on soil ecology. *Trends Ecol. Evol.* **2006**, *21*, 548–554. [CrossRef]
44. Kuzyakov, Y.; Gavrichkova, O. REVIEW: Time lag between photosynthesis and carbon dioxide efflux from soil: A review of mechanisms and controls. *Glob. Chang. Biol.* **2010**, *16*, 3386–3406. [CrossRef]
45. Reichle, D.E. *The Global Carbon Cycle and Climate Change: Scaling Ecological Energetics From Organism to the Biosphere*; Elsevier: Amsterdam, The Netherlands, 2020.
46. Reichstein, M.; Rey, A.; Freibauer, A.; Tenhunen, J.; Valentini, R.; Banza, J.; Casals, P.; Cheng, Y.; Grünzweig, J.M.; Irvine, J.; et al. Modeling temporal and large-scale spatial variability of soil respiration from soil water availability, temperature and vegetation productivity indices. *Glob. Biogeochem. Cycles* **2003**, *17*, 1104. [CrossRef]
47. Ma, Y.; Geng, Y.; Huang, Y.; Shi, Y.; Niklaus, P.A.; Schmid, B.; He, J. Effect of clear-cutting silviculture on soil respiration in a subtropical forest of China. *J. Plant Ecol.* **2013**, *6*, 335–348. [CrossRef]
48. Mayer, M.; Matthews, B.; Rosinger, C.; Sandén, H.; Godbold, D.L.; Katzensteiner, K. Tree regeneration retards decomposition in a temperate mountain soil after forest gap disturbance. *Soil Biol. Biochem.* **2017**, *115*, 490–498. [CrossRef]
49. Coleman, M.D.; Aubrey, D.P. Stand development and other intrinsic factors largely control fine-root dynamics with only subtle modifications from resource availability. *Tree Physiol.* **2018**, *38*, 1805–1819. [CrossRef]
50. Ruzol, R.; Staudhammer, C.L.; Younger, S.; Aubrey, D.; Loescher, H.W.; Jackson, C.R.; Starr, G. Water use from a young loblolly pine bioenergy plantation: Effects of intensive management on stand evapotranspiration. *Ecosphere* **2022**, *13*, e4100. [CrossRef]
51. Aubrey, D.P.; Teskey, R.O. Root-derived CO_2 efflux via xylem stream rivals soil CO_2 efflux. *New Phytol.* **2009**, *184*, 35–40. [CrossRef] [PubMed]
52. Aubrey, D.P.; Teskey, R.O. Xylem transport of root-derived CO_2 caused a substantial underestimation of belowground respiration during a growing season. *Glob. Chang. Biol.* **2021**, *27*, 2991–3000. [CrossRef] [PubMed]

53. Wu, Z.; Dijkstra, P.; Koch, G.W.; Peñuelas, J.; Hungate, B.A. Responses of terrestrial ecosystems to temperature and precipitation change: A meta-analysis of experimental manipulation. *Glob. Chang. Biol.* **2011**, *17*, 927–942. [CrossRef]
54. Xu, M.; Qi, Y. Soil-surface CO_2 efflux and its spatial and temporal variations in a young ponderosa pine plantation in northern California. *Glob. Chang. Biol.* **2001**, *7*, 667–677. [CrossRef]
55. Yuste, J.C.; Janssens, I.A.; Carrara, A.; Meiresonne, L.; Ceulemans, R. Interactive effects of temperature and precipitation on soil respiration in a temperate maritime pine forest. *Tree Physiol.* **2003**, *23*, 1263–1270. [CrossRef]
56. Hursh, A.; Ballantyne, A.; Cooper, L.; Maneta, M.; Kimball, J.; Watts, J. The sensitivity of soil respiration to soil temperature, moisture, and carbon supply at the global scale. *Glob. Chang. Biol.* **2017**, *23*, 2090–2103. [CrossRef]
57. Hawkes, C.V.; Waring, B.G.; Rocca, J.D.; Kivlin, S.N. Historical climate controls soil respiration responses to current soil moisture. *Proc. Natl. Acad. Sci. USA* **2017**, *114*, 6322–6327. [CrossRef]
58. Wiesner, S.; Staudhammer, C.L.; Loescher, H.W.; Baron-Lopez, A.; Boring, L.R.; Mitchell, R.J.; Starr, G. Interactions among abiotic drivers, disturbance and gross ecosystem carbon exchange on soil respiration from subtropical pine savannas. *Ecosystems* **2018**, *21*, 1639–1658. [CrossRef]
59. Oren, R.; Sperry, J.S.; Katul, G.G.; Pataki, D.E.; Ewers, B.E.; Phillips, N.; Schäfer, K.V.R. Survey and synthesis of intra- and interspecific variation in stomatal sensitivity to vapour pressure deficit. *Plant Cell Environ.* **1999**, *22*, 1515–1526. [CrossRef]
60. Novick, K.A.; Ficklin, D.L.; Stoy, P.C.; Williams, C.A.; Bohrer, G.; Oishi, A.C.; Papuga, S.A.; Blanken, P.D.; Noormets, A.; Sulman, B.N. The increasing importance of atmospheric demand for ecosystem water and carbon fluxes. *Nat. Clim. Change* **2016**, *6*, 1023–1027. [CrossRef]
61. Grossiord, C.; Buckley, T.N.; Cernusak, L.A.; Novick, K.A.; Poulter, B.; Siegwolf, R.T.W.; Sperry, J.S.; McDowell, N.G. Plant responses to rising vapor pressure deficit. *New Phytol.* **2020**, *226*, 1550–1566. [CrossRef] [PubMed]